Excitation Spectra of Donors in Aluminum Antimonide*

B. T. AHLBURN AND A. K. RAMDAS
Department of Physics, Purdue University, Lafayette, Indiana
(Received 30 October 1967)

The photoexcitation spectra associated with tellurium and selenium donors in aluminum antimonide have been studied. At liquid-helium temperatures, sharp lines are observed in the spectra associated with both donors. At liquid-nitrogen temperature, the lines of the tellurium spectrum broaden, whereas those of selenium vanish, being replaced by a broad region of continuous high absorption. For both tellurium and selenium donors, none of the above features are observed at 300°K. In each case, at photon energies higher than the donor ionization energy, absorption peaks have been observed which are consistent with their arising from electronic transitions accompanied by the emission of phonons. The effect of uniaxial stress has been studied for the excitation spectrum of both donors. On the basis of the absence of splittings of the selenium lines for compressive force **F** parallel to ⟨111⟩, it is deduced that the conduction-band minima occur along ⟨100⟩. On the basis of the number of stress-induced components and their dichroic properties, it is concluded that line 1 of the tellurium donor at 38.31 meV and line 1 of the selenium donor at 117.13 meV are due to a $1s(A_1) \rightarrow 1s(T_1)$ transition. Similarly, line 2 of the tellurium donor at 57.96 meV and line 2 of the selenium donor at 134.3 meV have been attributed to a $1s(A_1) \rightarrow 2p_0$ transition.

I. INTRODUCTION

THE study of the photoexcitation spectra of charge carriers bound to imperfections in semiconductors has yielded considerable information about the localized electronic states associated with them; to the extent that these states are described in terms of the band structure, such studies have been useful in understanding the properties of the host crystal. The imperfections which have been most extensively investigated from this point of view are the substitutional group-V donors and group-III acceptors in silicon and germanium.[1] Among the III–V compounds, only recently brief accounts of the excitation spectra associated with tellurium and selenium donors in aluminum antimonide,[2,3] and those associated with manganese acceptors in gallium arsenide[4] have appeared. In addition, acceptor excitation spectra have been observed in indium antimonide and gallium antimonide.[5] The object of the present paper is to report in detail the results of an investigation of the excitation spectra of tellurium and selenium donors in aluminum antimonide. The application of the piezospectroscopic technique has proved to be valuable in the study of impurity levels[6–15]; the results of such effects for the donor spectra of aluminum antimonide are also reported in this paper.

II. EXPERIMENTAL PROCEDURE

In the present investigation a Perkin-Elmer double-pass grating monochromator, Model 112 G, was used for most of the measurements. The results shown in Figs. 1 and 2 were obtained with a Perkin-Elmer single-pass grating monochromator, Model 210. Both monochromators were equipped with Bausch and Lomb plane blazed reflection gratings. A Reeder[16] thermocouple with either a cesium iodide or a diamond window was used as a detector. The optical cryostat used for the measurements has been described by Fisher *et al.*.[17] The optical samples of aluminum antimonide were obtained from single-crystal ingots grown by Bell and Howell.[18] The room-temperature carrier concentration of the tellurium-doped specimens ranged from 2×10^{16} to 5×10^{16} cm^{-3} while the selenium-doped samples had a room-temperature carrier concentration of $\sim10^{16}$ cm^{-3}. The samples used in stress measurements were oriented using x-rays. Special precautions were necessary in the preparation of optical samples of aluminum antimonide because of the tendency of the surfaces to deteriorate in air. The specimens were first lapped to the required thickness in a slurry of No. 3200 silicon-carbide grit and kerosene. They were next polished with 1-μ diamond paste and finally with $\frac{1}{4}$-μ diamond paste, using kerosene as a lubricant. When the polishing was completed the

* Work supported by Advanced Research Projects Agency and the U. S. Army Research Office, Durham.
[1] W. Kohn, in *Solid State Physics*, edited by F. Seitz and D. Turnbull (Academic Press Inc., New York, 1957), Vol. 5, p. 257.
[2] B. T. Ahlburn and A. K. Ramdas, Phys. Letters **22**, 261 (1966).
[3] B. T. Ahlburn and A. K. Ramdas, Bull. Am. Phys. Soc. **12**, 139 (1967).
[4] R. A. Chapman and W. G. Hutchinson, Phys. Rev. Letters **18**, 443 (1967).
[5] P. Fisher (private communication).
[6] R. L. Aggarwal and A. K. Ramdas, Phys. Rev. **137**, A602 (1965).
[7] R. L. Aggarwal and A. K. Ramdas, Phys. Rev. **140**, A1246 (1965).
[8] R. L. Aggarwal, P. Fisher, V. Mourzine, and A. K. Ramdas, Phys. Rev. **138**, A882 (1965).
[9] J. H. Reuszer and P. Fisher, Phys. Rev. **140**, A245 (1965).
[10] J. H. Reuszer and P. Fisher, Phys. Rev. **165**, 909 (1968).
[11] P. Fisher and A. K. Ramdas, Phys. Letters **16**, 26 (1965).
[12] P. Fisher, R. L. Jones, A. Onton, and A. K. Ramdas, J. Phys. Soc. Japan Suppl. **21**, 224 (1966).
[13] A. Onton, P. Fisher and A. K. Ramdas, Phys. Rev. **163**, 686 (1967).
[14] R. L. Jones and P. Fisher, Solid State Commun. **2**, 369 (1964).
[15] D. H. Dickey and J. O. Dimmock, J. Phys. Chem. Solids **28**, 529 (1967).
[16] Manufactured by Charles M. Reeder and Co., Inc., 196 Victor Avenue, Detroit 3, Mich.
[17] P. Fisher, W. H. Haak, E. J. Johnson, and A. K. Ramdas, in *Proceedings of the Eighth Symposium on the Art of Glassblowing* (The American Scientific Glassblowing Society, Wilmington, Delaware, 1963), p. 136.
[18] Bell and Howell Research Laboratories, 360 Sierra Madre Villa, Pasadena, Calif. 91109.

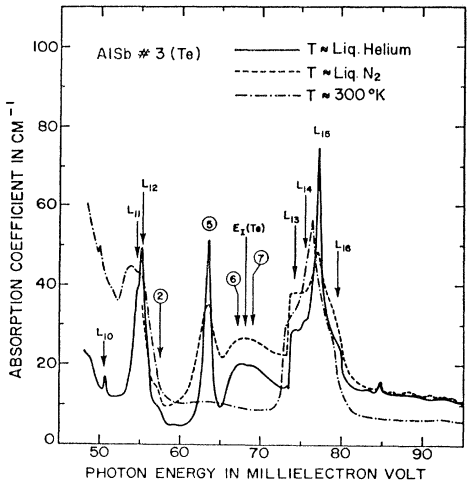

FIG. 1. The absorption spectra of tellurium donors in aluminum antimonide. Measurements were made at room temperature, as well as using liquid nitrogen and liquid helium as coolants. The room-temperature carrier concentration $n(300°K) \simeq 2\times10^{16}$ cm^{-3}.

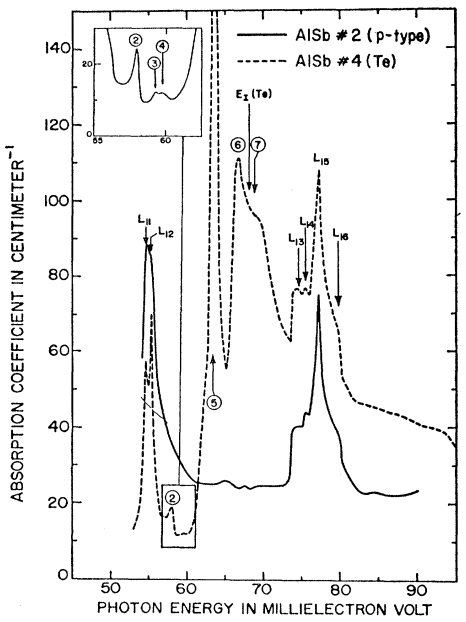

FIG. 2. The absorption spectra of a tellurium-doped sample of aluminum antimonide having $n(300°K) \simeq 5\times10^{16}$ cm^{-3} and of a p-type sample having $n(300°K) \simeq 3\times10^{16}$ cm^{-3}. Liquid helium was used as coolant.

samples were immediately transferred to the cryostat, which was then evacuated. In the stress studies uniaxial compression was applied using the thermal differential compression technique described by Rose-Innes.[6,19] Linearly polarized light used in the stress measurements was obtained with Perkin-Elmer wire grid transmission polarizers.[20] The excitation spectra of tellurium and selenium donors in aluminum antimonide lie mostly to the short-wavelength side of the reststrahlen band. The absorption coefficients in this range were calculated using the short-wavelength limit of the reflectivity, $R=0.260$.[21] The data shown in Figs. 3, 4, 8, and 10 include the range where the reflectivity shows a rapid variation with wavelength and hence the percent transmission rather than the absorption coefficient is presented as a function of photon energy.

III. EXPERIMENTAL RESULTS AND DISCUSSION: TELLURIUM DONORS

A. Zero Stress

The absorption spectra of a sample of tellurium-doped aluminum antimonide with a room-temperature carrier concentration of $\sim2\times10^{16}$ cm^{-3} are shown in Fig. 1; these have been obtained at room, liquid-nitrogen, and liquid-helium temperatures. In contrast to the multiphonon[21] absorption peaks denoted by L_{10}-L_{16}, the peaks 2, 5, 6, and 7 are observed only at the lower temperatures; they occur at 58.0, 63.5, 66.7, and 68.8 meV, respectively.[22] At room temperature the four peaks are not observed, but are replaced by a continuous absorption,[21,23] which increases monotonically with decreasing energy. The multiphonon lattice bands L_{10}-L_{16} shift slightly towards lower energies with increasing temperature. In Fig. 1 their positions at liquid-helium temperature are denoted. The results shown in Fig. 2 were obtained using a tellurium-doped specimen of a concentration higher than that used to obtain the results of Fig. 1; also shown are the results for a p-type specimen. As can be seen from Figs. 1 and 2, the lines

TABLE I. Energies of excitation lines observed in n-type aluminum antimonide.

Tellurium		Selenium	
Line number	Energy (meV)	Line number	Energy (meV)
1	38.31±0.03	1	117.13±0.05
2	57.96±0.04	2	134.3 ±0.2
3	59.2 ±0.1	3	135.7 ±0.5
4	59.7 ±0.1	4	138.7 ±0.2
5	63.5 ±0.1	5	142.4 ±0.3
6	66.7 ±0.5	6	146.3 ±0.5
7	68.8 ±0.5	7	157.3 ±1.0
8a	97.19±0.20	8	166.0 ±1.0
8b	97.86±0.20	9	175.4 ±0.3
9a	101.45±0.20	10	177.7 ±0.3
9b	102.15±0.20	11	180.8 ±0.5
10a	105.15±0.20	12	184.4 ±0.5
10b	105.91±0.20	13	194.6 ±1.0
11	108.2 ±0.2	14	199.0 ±2.0
X	43.71±0.06		

[19] A. C. Rose-Innes, Proc. Phys. Soc. (London) **72**, 514 (1958).
[20] The wire grid transmission polarizer has been described by G. R. Bird and M. Parrish, Jr., J. Opt. Soc. Am. **50**, 886 (1960). For wavelength regions below 18 μ, a polarizer having a AgCl substrate was used. For wavelength regions above 18 μ a polarizer having a polyethylene substrate was used. These polarizers were purchased from the Perkin-Elmer Corporation, Norwalk, Conn.
[21] W. J. Turner and W. E. Reese, Phys. Rev. **127**, 126 (1962).
[22] The peaks labeled I, II, III, and IV in Ref. 2 are here denoted by 2, 5, 6, and 7, respectively.
[23] W. J. Turner and W. E. Reese, Phys. Rev. **117**, 1003 (1960).

TABLE II. Energies of lattice bands in aluminum antimonide.

Line number	Energy (meV)
L_1[a]	29.7 ±0.1
L_2	35.56±0.04
L_3	36.8 ±0.1
L_4[b]	38.0 ±0.2
L_5[b]	38.6 ±0.1
L_6	40–42
L_7	45.6 ±0.1
L_8	47.49±0.04
L_9	48.6 ±0.2
L_{10}	50.6 ±0.1
L_{11}	54.55±0.04
L_{12}	55.24±0.04
L_{13}	74.4 ±0.3
L_{14}	75.4 ±0.2
L_{15}	77.15±0.04
L_{16}	79.6 ±0.2

[a] A line labeled L_1' appears at 29.2 meV in selenium-doped AlSb. The significance of the difference in the positions of L_1 and L_1' is not clear.
[b] Lines L_4 and L_5 apparently are masked by line 1 in tellurium-doped material.

2–7 of the tellurium donors are much stronger in the latter. The inset to Fig. 2 shows line 2 and the very weak lines 3 and 4 more clearly. The energies of lines of electronic origin are given in Table I. Lines attributed to lattice vibrations on the basis of their occurrence in tellurium-doped, selenium-doped, and p-type aluminum antimonide, or from their persistence at room temperature, are labeled L_1, $L_2\cdots$. Their energies are given in Table II. Also, as can be seen in Fig. 2, lines 2–7 do not occur in the spectrum obtained with p-type material. That these lines are characteristic of tellurium donors is further demonstrated by their absence in a selenium-doped sample whose transmission spectrum is shown in Fig. 3. The ionization energy of tellurium donors in aluminum antimonide has been measured electrically by Reid[24] to be 68 meV. This is very close to the position of peak 7. Thus the excitation spectrum associated with donor electrons should occur at energies below this value. From the experimental observations discussed above it is concluded that peaks 2–7 arise from photo-excitation of the donor electrons associated with tellurium impurity; line 7 could be attributed to a photo-ionization peak or to excitations to levels close to the conduction band. The gradual decrease of absorption beyond ~70 meV, clearly observable in Fig. 2, can be ascribed to photo-ionization of the tellurium donors, whereas the high level of background absorption between 58 and 70 meV seen in the p-type specimen appears to be associated with a shallow acceptor having an ionization energy ~33 meV.[25] The monotonically increasing absorption toward lower energies, observed at room temperature and shown in Fig. 1, is characteristic of free-carrier absorption.

[24] F. J. Reid, in *Compound Semiconductors*, edited by R. K. Willardson and H. L. Goering (Reinhold Publishing Corporation, New York, 1962), Vol. 1, p. 159.
[25] R. J. Stirn and W. M. Becker, Phys. Rev. **148**, 907 (1966). The high level of background absorption between 58 and 70 meV seen in the p-type specimen was first attributed to poor surfaces (see Ref. 2).

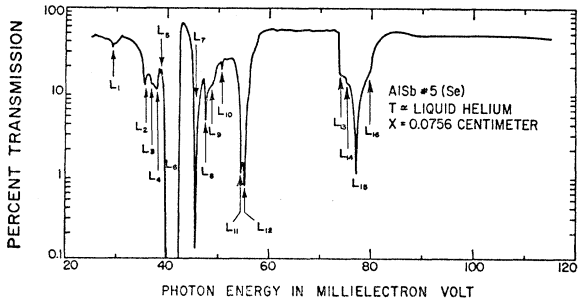

FIG. 3. The transmission spectrum of selenium-doped aluminum antimonide in the energy range 25–115 meV; $n(300°\text{K})\simeq 10^{16}$ cm^{-3}. Liquid helium was used as coolant.

In order to understand the localized electronic states giving rise to the excitation lines discussed above, it is of interest to consider the problem in the framework of the effective-mass theory as developed for shallow donors in silicon and germanium.[1] The nature of the lowest conduction-band minimum is an important feature in this approach. Recently it has been shown that aluminum antimonide has, like silicon, conduction-band minima along ⟨100⟩. This has been deduced by Ghanekar and Sladek on the basis of their piezoresistance and piezo-Hall-effect studies,[26] and by Stirn and Becker from their investigation of magnetoresistance.[27] The latter authors deduced from their measurements the following effective-mass values: $m_{\parallel}=(1.50\pm0.20)m_e$, and $m_{\perp}=(0.214\pm0.002)m_e$, where $m_{\parallel}$ and $m_{\perp}$ are the longitudinal and transverse effective masses and m_e is the free-electron mass. These values of the effective masses should be compared with the corresponding masses for silicon, $m_{\parallel}=0.98m_e$ and $m_{\perp}=0.19m_e$. It will be assumed that group-VI tellurium enters the aluminum antimonide lattice substitutionally, replacing group-V antimony atoms[28]; hence the site symmetry of the tellurium donors will be assumed to be T_d. Following the effective-mass theory for donors in silicon and germanium, the Schrödinger equation[29] for the donor electrons is

$$\left[-\gamma\frac{\partial^2}{\partial z^2}+\frac{\partial^2}{\partial x^2}+\frac{\partial^2}{\partial y^2}-\frac{2}{r}-\epsilon\right]F(\mathbf{r})=0, \qquad (1)$$

TABLE III. Binding energies for donor states in aluminum antimonide in the effective-mass approximation.

Level	$\epsilon/\epsilon_0(\kappa_0)$[a]	ϵ (meV)
$1s$	−1.76 ±0.14	−40.0 ±3.2
$2p_0$	−0.72 ±0.10	−16.3 ±2.2
$3p_0$	−0.38 ±0.05	− 8.6 ±1.1
$2p_{\pm}$	−0.342±0.010	− 7.76±0.23
$3p_{\pm}$	−0.172±0.011	− 3.91±0.25

[a] $\epsilon_0(\kappa_0)=22.7$ meV.

[26] K. M. Ghanekar and R. J. Sladek, Phys. Rev. **146**, 505 (1966).
[27] R. J. Stirn and W. M. Becker, Phys. Rev. **141**, 621 (1966).
[28] O. Madelung, *Physics of III–V Compounds* (John Wiley & Sons, Inc., New York, 1964), Chap. 5, p. 221.
[29] W. Kohn and J. M. Luttinger, Phys. Rev. **98**, 915 (1955).

TABLE IV. Energy spacings of excited donor states.

States	Calculated spacing (meV)	Spacing observed for tellurium (meV)	Spacing between lines...	Spacing observed for selenium (meV)	Spacing between lines...
$2p_{\pm}-1s(T_1)$	32.2±3.4	25.2±0.2	No. 5 and No. 1	21.6±0.3	No. 4 and No. 1
$2p_{\pm}-2p_0$	8.5±2.5	5.5±0.2	No. 5 and No. 2	4.4±0.5	No. 4 and No. 2
$2p_{\pm}-3p_0$	0.8±1.3	3.8±0.2	No. 5 and No. 4	3.0±0.5	No. 4 and No. 3
$3p_{\pm}-2p_{\pm}$	3.9±0.5	3.2±0.5	No. 6 and No. 5	3.7±0.5	No. 5 and No. 4

where $\gamma=m_{\perp}/m_{\parallel}$, $F(\mathbf{r})$ is the envelope function, $m_{\parallel}$ and $m_{\perp}$ are defined for a valley along [001], and ϵ, the energy, is in units of $\epsilon_0=m_{\perp}e^4/2\hbar^2\kappa^2$. Here κ is the dielectric constant. Unlike the case of the covalent semiconductors like silicon, for a partially ionic crystal like aluminum antimonide,[30] κ used in Eq. (1) may be frequency-dependent. If the binding energy of a given impurity state is much smaller than the optical phonon energies, the use of the static dielectric constant κ_0 is reasonable. In Table III are given the binding energies of the $1s$, $2p_0$, $2p_{\pm}$, $3p_0$, and $3p_{\pm}$ states calculated using κ_0. The values of ϵ/ϵ_0 shown in Table III were estimated graphically using the known values of ϵ/ϵ_0 for effective mass ratios $\gamma=1$ (hydrogenic limit), 0.19 (silicon), 0.051 (germanium), and 0 (adiabatic limit).[29] As can be seen from the table, the binding energy of the $1s$ state estimated in this manner is very close to the reststrahlen energy. Thus, for aluminum antimonide, the use of the static dielectric constant for the calculation of the binding energy of the $1s$ ground state needs justification. In addition, the mechanisms leading to the chemical splittings observed for the group-V donors in silicon[7] and germanium[31] will also be present. As in the case of silicon, the sixfold degeneracy of the $1s$ ground state can be expected to be partially lifted, leading to a singlet $1s(A_1)$, a doublet $1s(E)$ and a triplet $1s(T_1)$ state. The letters in parentheses denote the irreducible representations of the point group T_d, the site symmetry of the donor. Here the irreducible representations are labeled following the notation used by Kohn and Luttinger.[29] The singlet state is depressed *below* the effective-mass position for all the group-V donors in silicon whereas the $1s(E)$ and the $1s(T_1)$ levels have been found to be near the effective-mass position. For the interstitial lithium donor in silicon, however, the singlet level lies *above* the effective-mass position.[8] Anticipating the stress effects discussed in the next section, the lowest-ground state will be assumed to be the $1s(A_1)$. It should be noted from Table III that, with the value of $m_{\perp}/m_{\parallel}$ for aluminum antimonide, the binding energy of the $3p_0$ state is expected to lie between those for the $2p_0$ and $2p_{\pm}$ levels, as is the case for germanium. The spacings of the energy levels are compared with experimentally observed line spacings in Table IV. In this comparison, it is assumed that the most prominent line, line 5, corresponds to a transition to the $2p_{\pm}$ excited state, in analogy with the case of donors in silicon. The positions of lines 3 and 4 are close to that expected for the $1s(A_1)\rightarrow 3p_0$ transition. The agreement between the estimated and the observed values should be considered only fair; this is not surprising in view of the uncertainties present in the calculations and the experimentally determined line positions. It should be pointed out that the intensity of line 2, assigned to the $1s(A_1)\rightarrow 2p_0$ transition, relative to that of line 5, assigned to the $1s(A_1)\rightarrow 2p_{\pm}$ transition, is very small compared to the corresponding relative intensities in silicon. The ionization energy, E_I(Te), of the tellurium donors in aluminum antimonide can be calculated by adding to the experimentally observed energy of, for example, the $1s(A_1)\rightarrow 2p_{\pm}$ transition here ascribed to line 5, the calculated binding energy of the $2p_{\pm}$ excited state. This turns out to be 71.3±0.3 meV which is to be compared with the electrically determined value of 68 meV. A corresponding calculation using the high-frequency dielectric constant yields E_I(Te) = 74.6 meV. It thus appears that the use of the static dielectric constant gives a value for E_I(Te) closer to the experimentally observed value. It appears from such considerations that the optical ionization energy is close to the thermal-ionization energy. In fact, if line 7 is due to photo-ionization, this agreement is very close. In view of this there appears to be little Franck-Condon shift.[32]

Optical transitions have been reported for bismuth and sulfur impurities in silicon which have been attributed to $1s(A_1)\rightarrow 1s(T_1)$ transitions.[33–35] It is of interest to enquire if such transitions occur for donors in aluminum antimonide also. Such transitions are forbidden in the effective-mass approximation; also, in the effective-mass theory the $1s(A_1)$, $1s(E)$ and $1s(T_1)$ states have the same energy. With the failure of the effective-mass theory for the ground state, however, transitions between the ground states can occur. With the site symmetry of the donor as T_d, only the $1s(A_1)\rightarrow 1s(T_1)$ transition is allowed from group-theoretical considerations. In order to look for such a transition for

[30] O. Madelung, Ref. 28, Chap. 2, p. 22.
[31] J. H. Reuszer and P. Fisher, Phys. Rev. **135**, A1125 (1964).
[32] J. Markham, in *Solid State Physics*, edited by F. Seitz and D. Turnbull (Academic Press Inc., New York, 1966), Suppl. 8, Chap. 4, p. 124.
[33] W. E. Krag and H. J. Zeiger, Phys. Rev. Letters **8**, 485 (1962).
[34] W. E. Krag, W. H. Kleiner, H. J. Zeiger, and S. Fischler, J. Phys. Soc. Japan Suppl. **21**, 230 (1966).
[35] H. J. Zeiger, W. E. Krag, and L. M. Roth, MIT Lincoln Laboratory, Quarterly Report, Solid State Research, 1962, p. 28 (unpublished).

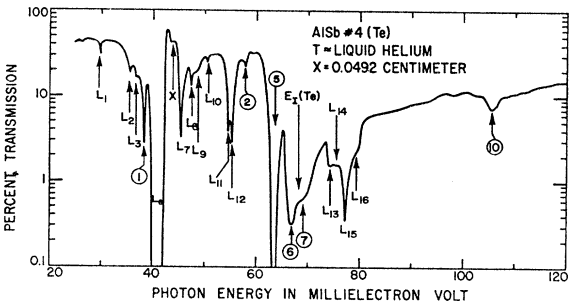

FIG. 4. The transmission spectrum of tellurium-doped aluminum antimonide in the energy range 25–120 meV; $n(300°K) \simeq 5\times10^{16}$ cm^{-3}. Liquid helium was used as coolant.

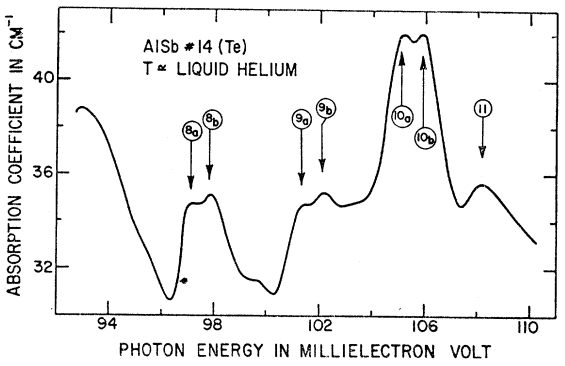

FIG. 5. Peaks observed in the absorption spectrum of tellurium-doped aluminum antimonide at energies greater than the donor-ionization energy; $n(300°K) \simeq 5\times10^{16}$ cm^{-3}. Liquid helium was used as coolant.

tellurium donors in aluminum antimonide, the absorption spectrum was extended to 24 meV. The results are presented in Fig. 4. The spectrum of selenium-doped aluminum antimonide in the same range is presented in Fig. 3. A number of lines labeled L_1, L_2, L_3, 1, L_6, X, L_7-L_{10} occur in the tellurium-doped specimen; in the selenium-doped specimen besides L_2, L_3, and L_6-L_{10}, a weak line labeled L'_1 close to L_1, and weak lines labeled L_4 and L_5 close to line 1 have been observed. The lines L_6, L_7, and L_8 have been reported previously.[21] Besides the lines mentioned above ,the data presented in Fig. 3 and Fig. 4 show additional features for the lattice bands around 55 and 78 meV. As can also be seen in Fig. 2, a clearly resolved doublet is observed with peaks at 54.55 (L_{11}) and 55.24 (L_{12}) meV; there is also some evidence for a shoulder on the high-energy side of this band. These correspond to the absorption peak at 54.4 meV in the measurements of Turner and Reese.[21] Also, the lattice band near 78 meV shows four components at helium temperature, as can be seen in Figs. 1–4. In Fig. 1 it is seen that only three peaks are observable at liquid-nitrogen and room temperatures, in agreement with the observations of Turner and Reese.

Among the above lines, lines 1 and X appear to be unique to the tellurium spectrum. The interpretation of line 1 as an electronic transition associated with the tellurium donor will be supported by the stress results presented in the following section. If line 1 is indeed due to the $1s(A_1) \rightarrow 1s(T_1)$ transition, this would indicate that the $1s(T_1)$ level has a binding energy of $[E_I(\mathrm{Te}) - 38.3] \approx 30$ meV, in contrast to $\sim$40 meV estimated for the effective-mass ground state in Table III. It should also be noted that line 1 is fairly intense in contrast to the $1s(A_1) \rightarrow 1s(T_1)$ transitions observed previously for bismuth-doped silicon.[33,35] A comparison of the separation between lines 5 and 1, $[63.5-38.3] = 25.2$ meV, with the estimated spacing between the $2p_\pm$ and $2p_0$ levels, 8.5 ± 2.5 meV, rules out the possibility of line 1 arising from a $1s(A_1) \rightarrow 2p_0$ transition on the basis of the present model. The interpretation of the very weak line X is not clear.

In Figs. 4 and 5 it may be seen that at helium temperature several peaks occur in tellurium-doped aluminum antimonide at energies substantially greater than $E_I(Te)$. They do not appear in selenium-doped material (see Fig. 3) or at room temperature in tellurium-doped samples. Hence the peaks labeled 8, 9, 10, and 11, occurring at 97.5, 101.8, 105.6, and 108.2 meV, respectively, are clearly associated with the tellurium impurity. The lines 8, 9, and 10 appear to be close doublets as can be seen in Fig. 5. This has been verified in several measurements. The positions given above are their mean positions. The most prominent of these lines, line 10, can be interpreted as arising from the $1s(A_1) \rightarrow 2p_\pm$ transition attributed to the strongest excitation line, line 5, at 63.5 meV and the simultaneous emission of a zone center LO_Γ phonon having an energy of 42.7 meV.[36] Tentative assignments for the lines 8–11 are given in Table V. Although the positions

TABLE V. Energies of electronic excitations accompanied by phonon emission.[a]

Line number	Energy (meV)	Tentative assignment	Calculated energy (meV)
		Tellurium donors	
8a	97.19	Line 2+TO$_\Gamma$	98.05
8b	97.86		
9a	101.45	Line 2+LO$_\Gamma$	100.66
9b	102.15		
10a	105.15	Line 5+LO$_\Gamma$	106.2
10b	105.91		
11	108.2	Line 7+TO$_\Gamma$	108.89
		Selenium donors	
7	155–159	Line 1+TO$_\Gamma$	157.2
		Line 1+LO$_\Gamma$	159.8
8	166		
9	175.4		
10	177.7	Line 4+TO$_\Gamma$	178.8
11	180.7	Line 4+LO$_\Gamma$	181.4
12	184.5	Line 5+LO$_\Gamma$	185.1
13	194.6		
14	199	Line 1+LO$_\Gamma$+TO$_\Gamma$	199.9

[a] The phonon energies used in the assignments are: TO$_\Gamma$ = 40.09 meV and LO$_\Gamma$ = 42.70 meV, respectively, measured at helium temperature (see Ref. 36). No assignments have been given for lines 8, 9, and 13 of the selenium spectrum; these lines do, however, lie in the range consistent with combinations with zone-boundary phonons given by Turner and Reese (see Ref. 21).

[36] A. Mooradian and G. Wright, Solid State Commun. 4, 431 (1966).

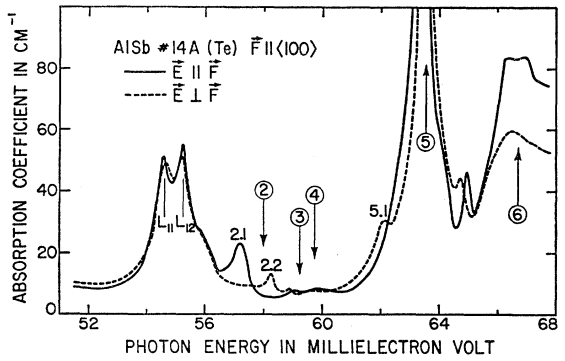

FIG. 6. Excitation spectrum of tellurium in aluminum antimonide with compressive force **F** along ⟨100⟩; $n(300°\text{K}) \simeq 5\times10^{16}$ cm^{-3}. Liquid helium was used as coolant.

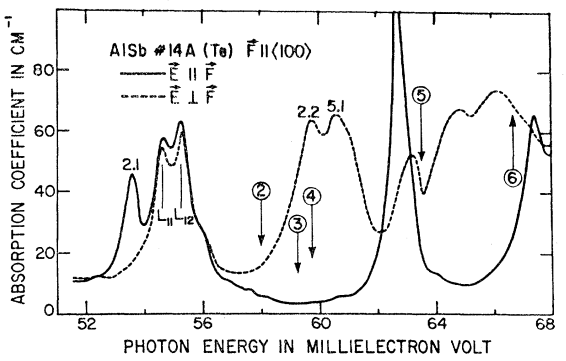

FIG. 7. Excitation spectrum of tellurium in aluminum antimonide with compressive force **F** along ⟨100⟩; $n(300°\text{K}) \simeq 5\times10^{16}$ cm^{-3}. Liquid helium was used as coolant. The stress for this case is greater than that in Fig. 6.

of lines 8 and 9 are consistent with their interpretations as arising from the transition giving rise to line 2 accompanied by the emission of a TO_Γ and an LO_Γ phonon, respectively, their intensities relative to line 10 are somewhat higher than might be expected considering the relative intensities of lines 2 and 5. Many examples of electronic transitions between localized levels accompanied by the emission of optical phonons have been reported in the literature. For example, such transitions have been observed for an acceptor in semiconducting diamond by Smith and Taylor[37] and for manganese impurities in gallium arsenide by Chapman and Hutchinson.[4] Hardy has treated theoretically this type of transition for acceptors in diamond assuming that the bound holes and the phonons interact through an optical deformation potential.[38] Hopfield has examined the problem in polar materials assuming that the electrons or holes interact with the electric polarization field associated with the LO phonons.[39] Both approaches appear to be consistent with the observed relative intensities of lines 5 and 10. The origin of the doublet nature of 8, 9 and 10 is not at present clear.

Recently the question of impurity states associated with subsidiary conduction-band minima has been the subject of theoretical[40,41] and experimental investigations.[42] The possibility that some or all of the lines observed at energies greater than E_I(Te) arise from localized states associated with subsidiary minima must be considered here. The minima which might contribute most probably to the post-ionization absorption in tellurium-doped aluminum antimonide appear to be either the ⟨111⟩ minima, deduced by Mead and Spitzer[43] to be the next highest minima, or the X_3 (Δ_3) conduction-band minima, inferred by Cardona *et al.*[44] to lie along ⟨100⟩, ~0.36 eV above the X_1, the lowest conduction-band minima. Although this interpretation for lines 8–11 cannot be ruled out, it appears surprising, on this basis, that no lines are observed at energies greater than that of line **11**.

B. Effects of Uniaxial Stress

The effects of a compressive force **F** along ⟨100⟩ on the excitation lines 2–6 of tellurium donors in aluminum antimonide are shown in Figs. 6 and 7; the experimental conditions were such that the stress for Fig. 6 is smaller than for Fig. 7. The effect of **F**‖⟨100⟩ on line **1** is shown in Fig. 8; this was obtained in the same measurement as that shown in Fig. 6. Results, not reproduced here, were also obtained for several stresses intermediate to those of Figs. 6 and 7. It has been possible to assign unambiguously the stress-induced components of lines **1** and **2**, as these lines are sharp and well separated from the other excitation lines. On the other hand, the lines at higher energies, viz., lines 5 and 6, are not well

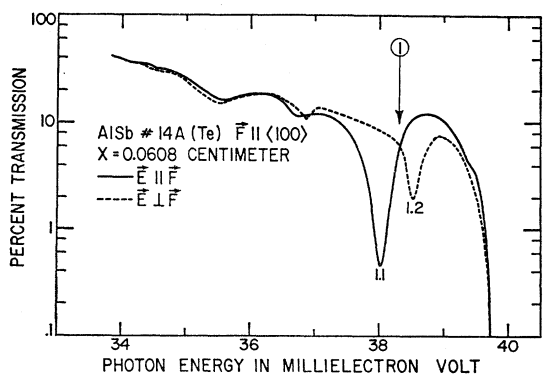

FIG. 8. The effect of a compressive force **F** along ⟨100⟩ on line 1 of the tellurium excitation spectrum. The magnitude of the stress and the sample are the same as in Fig. 6.

[37] S. D. Smith and W. Taylor, Proc. Phys. Soc. (London) **79**, 1142 (1962).
[38] J. R. Hardy, Proc. Phys. Soc. (London) **79**, 1154 (1962).
[39] J. J. Hopfield, J. Phys. Chem. Solids **10**, 110 (1959).
[40] G. A. Peterson, in *Proceedings of the International Conference on the Physics of Semiconductors, Paris, 1964* (Dunod Cie., Paris, 1964), p. 771.
[41] H. Kaplan, J. Phys. Chem. Solids **24**, 1593 (1963).
[42] B. B. Kosicki, W. Paul, A. J. Strauss, and G. W. Iseler, Phys. Rev. Letters **17**, 1175 (1966).
[43] C. A. Mead and W. G. Spitzer, Phys. Rev. Letters **11**, 358 (1963).
[44] M. Cardona, F. H. Pollak, and K. L. Shaklee, Phys. Rev. Letters **16**, 644 (1966).

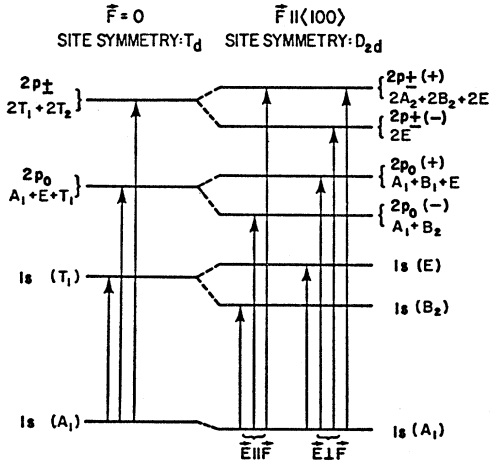

FIG. 9. Energy levels (not to scale) for $\mathbf{F}=0$ and $\mathbf{F}\|\langle 100\rangle$. The arrows indicate transitions allowed by group theory with the singlet $1s(A_1)$ as the ground state. The letters next to a level denote the effective-mass designation of the state and the irreducible representations of the appropriate site symmetry. Here the notation is the same as that used in Ref. 6.

resolved even in the absence of stress, and it has not been possible to associate the stress-induced components with the zero-stress lines. The only exception is the low-energy component labeled 5.1 which can be ascribed to line 5. The selection rules for $\mathbf{F}\|\langle 100\rangle$ are shown in Fig. 9. The results for $\mathbf{F}\|[110]$, $\mathbf{q}\|[001]$ are shown in Figs. 10 and 11; here $\mathbf{q}$ denotes the direction of light propagation. For this direction of compressive force, the stress-induced components originating from lines 1 and 2 can again be identified with certainty. Also the line labeled 5.1 appears to originate from line 5. The selection rules for $\mathbf{F}\|[110]$ are shown in Fig. 12.

Both for $\mathbf{F}\|\langle 100\rangle$ and $\mathbf{F}\|\langle 110\rangle$ the number of stress-induced components associated with lines 1 and 2, as well as their dichroism, is consistent with their assignments to $1s(A_1)\rightarrow 1s(T_1)$ and $1s(A_1)\rightarrow 2p_0$, respectively. These conclusions are based on the predictions of deformation-potential theory and group theory[6] that, for $\mathbf{F}\|\langle 100\rangle$, one component above the zero-stress

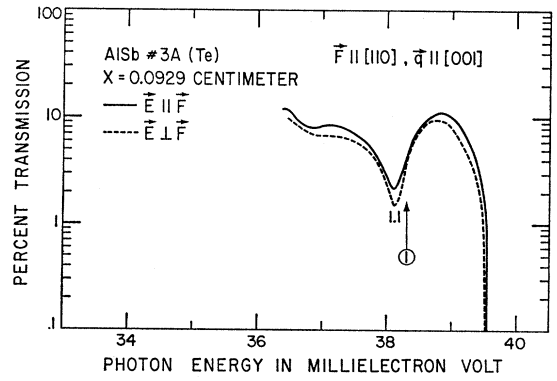

FIG. 10. The effect of $\mathbf{F}\|[110]$ on the excitation spectrum of tellurium, with light propagation vector $\mathbf{q}$ along [001]; $n(300°\text{K})\simeq 2\times 10^{16}$ cm^{-3}. Liquid helium was used as coolant.

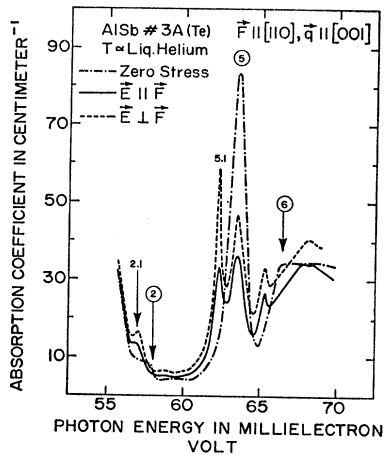

FIG. 11. The excitation spectrum of tellurium donors for $\mathbf{F}\|[110]$, $\mathbf{q}\|[001]$. Also shown is the zero-stress spectrum of the same sample; $n(300°\text{K})\simeq 2\times 10^{16}$ cm^{-3}. Liquid helium was used as coolant.

position for the electric vector $\mathbf{E}$ perpendicular to $\mathbf{F}$, and one component below the zero-stress position for $\mathbf{E}\|\mathbf{F}$ are expected for both these transitions. For $\mathbf{F}\|[110]$, $\mathbf{q}\|[001]$, only one component, occurring below the zero-stress position for both polarizations, is expected. In addition, the component 5.1 behaves like the low-energy component of a $1s(A_1)\rightarrow 2p_\pm$ transition for both directions of stress. Since both aluminum antimonide and silicon have conduction-band minima along $\langle 100\rangle$, the same stress behavior may be expected for donors in both crystals, which is indeed the case for lines 1 and 2. Using the present model, however, the interpretation of the components at energies above that of 5.1 is not clear.

In Fig. 7, the component 2.2 has been labeled as such on the basis of its polarization and its separation from

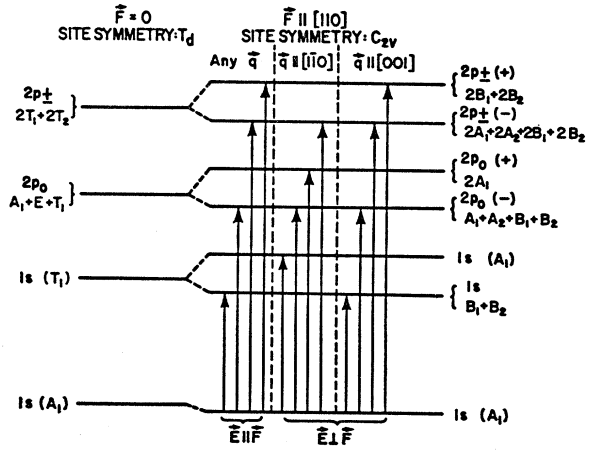

FIG. 12. Energy levels (not to scale) for $\mathbf{F}=0$ and $\mathbf{F}\|[110]$. The arrows represent the transitions allowed by group theory for $\mathbf{E}\|\mathbf{F}$, and all $\mathbf{q}$'s, and for $\mathbf{E}\perp\mathbf{F}$, $\mathbf{q}\|[110]$, and $\mathbf{q}\|[001]$. Though allowed by group theory, an intensity calculation shows that the $1s(A_1)\rightarrow 2p_0(-)$ transition for $\mathbf{q}\|[1\bar{1}0]$ and $\mathbf{E}\perp\mathbf{F}$ is forbidden (see Ref. 6).

the zero-stress position of line 2. Its intensity, is, however, somewhat higher than expected on the basis of the intensity of line 2. For $\mathbf{F}\|\langle 100\rangle$, the high donor concentration of the sample which was available results in an absorption so large that the behavior of lines 5, 6. . . could not be observed in full detail. Even for $\mathbf{F}\|\langle 110\rangle$, where the donor concentration of the sample used was low enough to resolve the stress-induced components around line 5, it has not been possible to assign the component which coincides with the zero-stress position of line 5 and the higher-lying components to given zero-stress lines. In the case of donors in silicon,[6] all lines split by the same amount for a given stress. This allowed the splitting of the $1s(A_1)\rightarrow 2p_0$ line to be used as a criterion in the assignment of the higher-lying stress components. In the present case, lines 1 and 2 split by different amounts; hence no such criterion is available. In addition, the low-energy and high-energy stress components of donor lines in silicon split away from their zero-stress positions in the ratio 2:1 for $\mathbf{F}\|\langle 100\rangle$, as is predicted by the group theory and deformation-potential theory. This is not observed even for lines 1 and 2 for the tellurium donors; this indicates that the various donor levels do not follow the conduction-band minima rigidly, contrary to the assumption of the theory. According to the theory no splittings are to be expected for $\mathbf{F}\|\langle 111\rangle$ if the conduction-band minima lie along $\langle 100\rangle$. This has been demonstrated for donors in silicon.[6] Such an experiment could not be carried out for tellurium donors in aluminum antimonide as a suitable sample was not available. It should be mentioned here that in the above discussion, stress-induced changes in the dielectric constant and the effective-mass parameters have been ignored for the stresses used in the present work; the results of similar experiments in silicon[6] and germanium[9] suggest that this assumption is reasonable. It has not been possible to attribute the comparative lack of success of the deformation potential and effective-mass approach in describing the stress behavior of tellurium donor states in aluminum antimonide to either the existence of complex donor centers or contributions from subsidiary conduction-band minima to the donor wave functions. It should be pointed out that the high concentration of donors in the samples of aluminum antimonide used in these measurements[45] may lead to interactions with nearby impurities. It is not clear to what extent the lack of details in the range where lines 5, 6, 7, etc. lie is due to this factor.

Attention should be drawn here to the fact that aluminum antimonide, a crystal with zinc blende structure of point group T_d, should, in principle, be piezoelectric. It is thus of importance to examine the contribution of the piezoelectric field to the piezospectroscopic effects. The piezoelectric effect need be considered only for $\mathbf{F}\|\langle 111\rangle$ and $\mathbf{F}\|\langle 110\rangle$, since it

[45] Stirn and Becker have determined $N_D\simeq 1.7\times 10^{17}$ cm^{-3} for Bell and Howell ingot No. 34 from which samples AlSb No. 4 and AlSb No. 14 were cut. See Ref. 27.

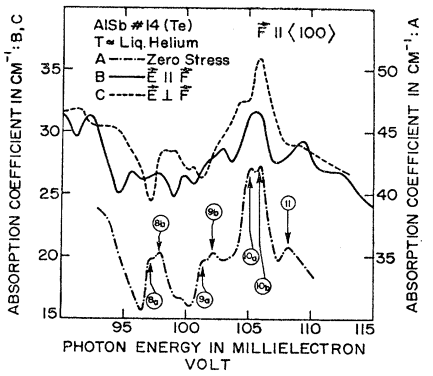

FIG. 13. Behavior of high-energy lines in tellurium-doped aluminum antimonide for $\mathbf{F}\|\langle 100\rangle$. The zero-stress spectrum is shown for the same sample; $n(300°\text{K})\simeq 5\times 10^{16}$ cm^{-3}. Liquid helium was used as coolant.

vanishes for $\mathbf{F}\|\langle 100\rangle$. The piezoelectric constant of aluminum antimonide does not appear to have been measured. The only nonzero-piezoelectric constant e_{14} can, however, be estimated using the following expression due to Born[46]

$$e_{14}^2=(\kappa_0-\kappa_\infty/4\pi)(C_{12}-C_{44})(C_{44}/C_{12}), \qquad (2)$$

where κ_0 and κ_∞ are the static and high-frequency dielectric constants, respectively, and C_{12} and C_{44} are the elastic stiffness constants. Using the values of Bolef and Menes[47] for C_{12} and C_{44} and of Turner and Reese[21] for κ_0 and κ_∞, piezoelectric fields of the order of 3×10^3 V/cm can be expected for stresses $\sim 10^8$ dyn/cm^2. Thus for $\mathbf{F}\|\langle 110\rangle$, the possibility of Stark effect has to be considered. As discussed above, the stress effects on lines 1 and 2 can be understood in the framework of the deformation-potential theory in so far as the number of stress-induced components and their dichroism is concerned. In the experimental set up used in the present investigations, it appears that the piezoelectric field is shorted out. Clearly, more definitive experiments are necessary to clarify this point.

Measurements on line 1 for stresses of different magnitudes have shown that it vanishes as the stress is increased, leaving a spectrum around 38 meV quite similar to that observed in selenium-doped aluminum antimonide. The vanishing of line 1 may be due to a resonance broadening which can occur when the energy separation between the states participating in the transition is equal to that of an optical phonon. This is similar to the behavior and interpretation for the $1s(A_1)\rightarrow 2p_0$ line of bismuth donors and line 2 of gallium acceptors in silicon.[48]

As can be seen from Fig. 13, lines 8a–11 which have been attributed to electronic excitation plus the emission

[46] M. Born, in *Encyklopadie der Mathematischen Wissenschaften*, edited by A. Sommerfeld (Verlag und Druck von B. G. Teubner, Leipzig, 1926), Vol. 5, Part 3, Chap. 25, p. 527.

[47] D. I. Bolef and M. Menes, J. Appl. Phys. **31**, 1426 (1960).

[48] A. Onton, P. Fisher, and A. K. Ramdas, Phys. Rev. Letters **19**, 781 (1967).

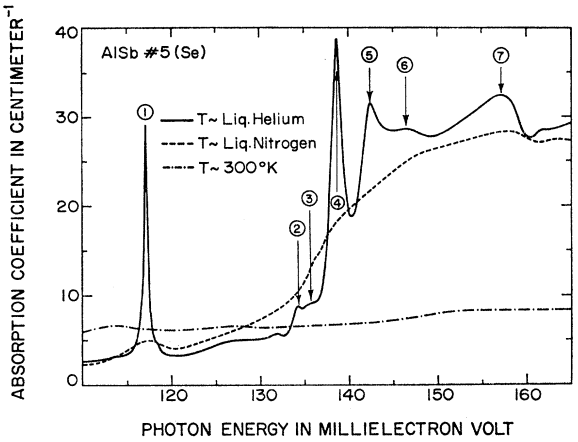

FIG. 14. The absorption spectra of selenium donors in aluminum antimonide. Measurements were made at room temperature as well as using liquid nitrogen and liquid helium as coolants; $n(300°K) \simeq 10^{16}$ cm^{-3}.

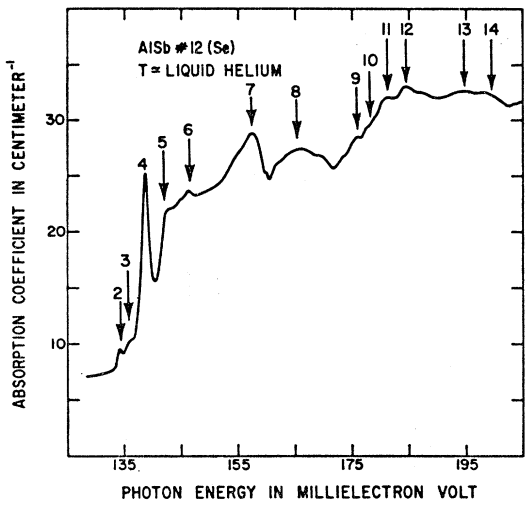

FIG. 15. The spectrum of selenium donors in aluminum antimonide including energies greater than the donor-ionization energy; $n(300°K) \simeq 10^{16}$ cm^{-3}. Liquid helium was used as coolant.

of optical phonons show a very complex behavior for $\mathbf{F} \| \langle 100 \rangle$. Although it has not been possible to interpret the stress results, the fact that the lines do split for $\mathbf{F} \| \langle 100 \rangle$ indicates that they do not arise from transitions associated solely with the $\langle 111 \rangle$ conduction-band minima.

IV. EXPERIMENTAL RESULTS AND DISCUSSION: SELENIUM DONORS

A. Zero Stress

The absorption spectra of selenium-doped aluminum antimonide with a room-temperature carrier concentration $\sim 10^{16}$ cm^{-3} are shown in Figs. 14 and 15. The ionization energy of selenium donors in aluminum antimonide has been reported to be $E_I(\mathrm{Se}) = 0.16$ eV.[25] The lines labeled 1–7 in Fig. 14 are thus in the range expected for the excitation lines associated with selenium donors; the positions of the lines are listed in Table I. Their absence in room-temperature measurements as well as in p-type and tellurium-doped material measured in the same energy range supports this interpretation. At liquid-nitrogen temperature lines 1–7 vanish, although large absorption does set in close to the region where lines 2–7 occur at helium temperature. The spectrum at liquid-nitrogen temperature is similar to that reported by Turner and Reese.[23] The nature of the spectrum associated with selenium donors at liquid-nitrogen temperature thus differs from that of the tellurium donors measured at the same temperature (compare Figs. 1 and 14). The origin of this difference is not clear.

If the most prominent line in the excitation spectrum of selenium donors, line 4, is ascribed to a $1s(A_1) \rightarrow 2p_\pm$ transition, the reasonable assignments for lines 1, 2, 3 and 5 are $1s(A_1) \rightarrow 1s(T_1)$, $1s(A_1) \rightarrow 2p_0$, $1s(A_1) \rightarrow 3p_0$, and $1s(A_1) \rightarrow 3p_\pm$, respectively. The spacing of the lines are given in Table IV, where the corresponding spacings in the effective-mass calculation and for tellurium donors are also presented. It is apparent from this table that agreement between the calculated and the observed spacings, as in the case of the tellurium donors, is somewhat poor.

The ionization energy, $E_I(\mathrm{Se})$, calculated, as in the case of tellurium donors, by adding the effective-mass value for the binding energy of the $2p_\pm$ state to the energy of line 4 turns out to be ~ 146.5 meV. This is significantly lower than the electrically determined value of ~ 160 meV. It is not clear whether or not this discrepancy is within the experimental accuracy of the electrical determination. If the ionization energy is taken to be 160 meV, the $1s(A_1) \rightarrow 2p_0$ transition should occur at ~ 144 meV. Thus no simple interpretation can be given for lines 2–5. However line 1 can be attributed to the $1s(A_1) \rightarrow 1s(T_1)$ transition accepting this value of the ionization energy; the binding energy of the $1s(T_1)$ level would then be ~ 43 meV, which is close to the effective-mass value, but substantially higher than the 30.7 meV deduced for the tellurium spectrum. On the other hand, if the ionization energy of the selenium donors is assumed to be 146.5 meV, the binding energy of the $1s(T_1)$ level turns out to be ~ 29.4 meV. Since the binding energy of the $1s(T_1)$ level may be expected to be essentially species-independent, the ionization energy of ~ 146.5 meV is thus to be preferred. For group-V donors in silicon and germanium, both theory[49] and experiment[7,31] do indicate that the $1s(T_1)$ level is essentially species-independent.

It can also be seen in Figs. 14 and 15, that there is a a strong absorption continuum beyond 150 meV extending up to ~ 200 meV; this is followed by a gradual falloff (not shown in the figures) towards higher

[49] A. Morita and H. Nara, J. Phys. Soc. Japan Suppl. **21**, 234 (1966).

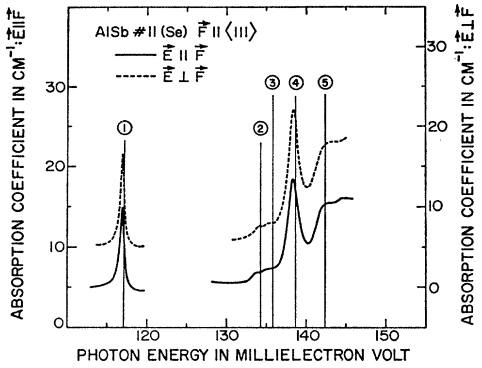

FIG. 16. Excitation spectrum of selenium donors in aluminum antimonide for $\mathbf{F}\|\langle 111\rangle$; $n(300°\mathrm{K})\simeq 10^{16}$ cm^{-3}. Liquid helium was used as coolant.

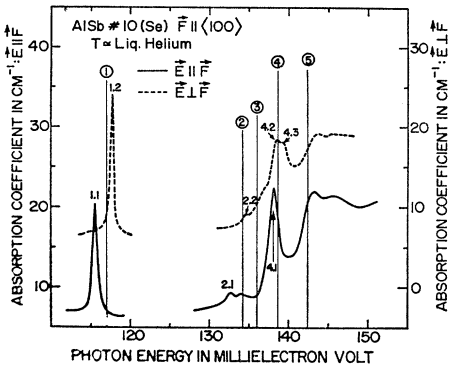

FIG. 17. Excitation spectrum of selenium donors in aluminum antimonide for $\mathbf{F}\|\langle 100\rangle$; $n(300°\mathrm{K})\simeq 10^{16}$ cm^{-3}. Liquid helium was used as coolant.

energies. Superimposed upon this continuum are many broad absorption peaks. As in the case of the tellurium donors, these absorption peaks may again be considered as arising either from electronic excitations accompanied by phonon emission or from transitions to levels associated with higher-lying conduction-band minima. Here again there is little evidence either to rule out or to support the latter interpretation. However, many of the peaks occur at energies close to those expected for various electronic excitation and phonon-emission combinations. For example, line 11 may be attributed to the $1s(A_1)\rightarrow 2p_\pm$ transition, line 4, of the selenium donor accompanied by the emission of a zone center LO phonon. In this respect it is the exact counterpart of line 10 in the tellurium-donor spectrum. The positions and assignments of several of the more prominent peaks in the energy range above E_I(Se) are given in TableV. It should be noted that one of the assignments invokes the emission of two phonons.

B. Effects of Uniaxial Stress

The behavior of the excitation spectrum of selenium donors under the application of a compressive force $\mathbf{F}\|\langle 111\rangle$ is shown in Fig. 16. The absence of splittings for lines 1–4 provides strong proof of the ⟨100⟩ nature of the lowest conduction-band minima. However, lines 1–4 do shift slightly towards lower energy. This implies that the ground state shifts slightly relative to the excited states. This feature is not expected on the basis of the effective-mass theory and the deformation-potential theory.[6] The possible contribution of the piezoelectric field has not yet been evaluated.

The effects of $\mathbf{F}\|\langle 100\rangle$ on lines 1–5 are shown in Fig. 17. As can be seen, line 1 clearly shows a low-energy component for $\mathbf{E}\|\mathbf{F}$ and a high-energy component for $\mathbf{E}\perp\mathbf{F}$; these components are labeled 1.1 and 1.2, respectively. This behavior is consistent with the line being due to either a $1s(A_1)\rightarrow 1s(T_1)$ or to a $1s(A_1)\rightarrow 2p_0$ transition. The selection rules for $\mathbf{F}\|\langle 100\rangle$ are shown in Fig. 9. In view of the discussion in the preceding section this evidence is interpreted as supporting the former assignment. The weak line 2 exhibits a similar pattern; this has been established on the basis of several measurements. Thus in view of the above observations, line 2 can be assigned to the $1s(A_1)\rightarrow 2p_0$ transition. Here again the low- and high-energy components of lines 1 and 2 do not split in the expected ratio of 2:1 about their zero-stress positions. The interpretation here is the same as in the case of the tellurium donors, i.e., the levels giving rise to lines 1 and 2 move differently relative to the conduction-band minima. Little can be said about the stress behavior of the weak line 3 which occurs as a shoulder on the low-energy side of the zero-stress position of line 4. A comparison of Figs. 14 and 17 suggests that the lines labeled 4.1, 4.2, and 4.3 in Fig. 17 arise from line 4 of the zero-stress spectrum. The difference in energy between lines 4.1 and 4.2 is greater than the experimental uncertainty of their determination. Hence it appears that line 4 splits into at least three components; this is contrary to the prediction of the effective-mass theory that each transition from the $1s(A_1)$ to the p-like states splits into two components. Even if lines 4.1 and 4.2 were to be regarded as the same low-energy component observed in both polarizations, the polarization pattern would be inconsistent with that predicted by theory for either a $1s(A_1)\rightarrow p_0$ or a $1s(A_1)\rightarrow p_\pm$ transition.

In Fig. 18 the behavior of lines 1 and 2 for $\mathbf{F}\|[110]$, $\mathbf{q}\|[001]$ is again consistent with their arising from the $1s(A_1)\rightarrow 1s(T_1)$ and the $1s(A_1)\rightarrow 2p_0$ transition, respectively. However, line 4 appears to show only one component which appears in both polarizations below the zero-stress position. Moreover, it appears to shift from its zero-stress position less than do the components of lines 1 and 2 from their respective zero-stress positions. The large breadth of line 4, and possibly its smaller splitting under stress make it difficult to ascertain whether or not line 4 actually splits into the two components expected for a $1s(A_1)\rightarrow 2p_\pm$ line (see Fig. 12). Also a comparison of Figs. 11 and 18 shows that line 4 of the selenium spectrum and line 5 of the tellurium spectrum behave quite differently for this

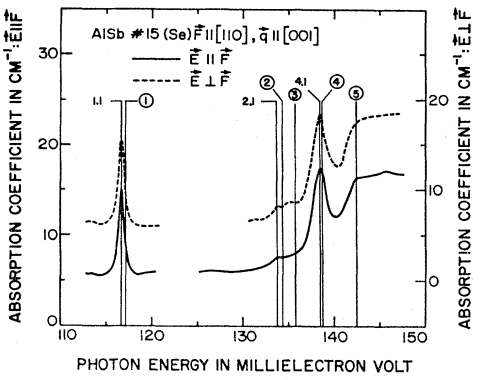

FIG. 18. Excitation spectrum of selenium donors in aluminum antimonide for $\mathbf{F}\|[110]$, $\mathbf{q}\|[001]$; $n(300°\mathrm{K})\simeq 10^{16}$ cm^{-3}. Liquid helium was used as coolant.

direction of stress and light propagation, although both lines have been ascribed to the $1s(A_1) \rightarrow 2p_{\pm}$ transition. Thus it is clear that a satisfactory understanding of these lines has not been reached in the present study.

In Fig. 19 the results for $\mathbf{F}\|[110]$, $\mathbf{q}\|[1\bar{1}0]$ on lines 1–4 are shown. Both lines 1 and 2 show a low-energy component for $\mathbf{E}\|\mathbf{F}$ and a high-energy component for $\mathbf{E}\perp\mathbf{F}$. This also is consistent with lines 1 and 2 arising from the $1s(A_1) \rightarrow 1s(T_1)$ and $1s(A_1) \rightarrow 2p_0$ transitions, respectively. It appears that the splitting of line 4 is smaller than the experimental uncertainty, so that again it has not been possible to interpret the stress behavior of line 4 as characteristic of either a $1s(A_1) \rightarrow p_0$ or a $1s(A_1) \rightarrow p_{\pm}$ transition. For this direction of compression and light propagation it is expected that spacings of the low-energy and high-energy components about the zero-stress position should be in the ratio of 1:2. Although the low-energy components of lines 1 and 2 do lie closer to the zero-stress position than the high-energy components, the ratio of the spacings is larger than 1:2.

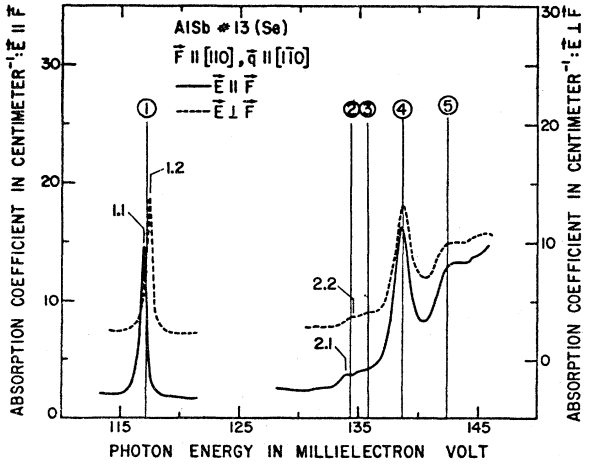

FIG. 19. Excitation spectrum of selenium donors in aluminum antimonide for $\mathbf{F}\|[110]$, $\mathbf{q}\|[1\bar{1}0]$; $n(300°\mathrm{K})\simeq 10^{16}$ cm^{-3}. Liquid helium was used as coolant.

V. DISCUSSION

The experimental results presented in this paper have established the existence of bound states for donor electrons in aluminum antimonide. It is of interest to compare the binding energies of donor electrons in aluminum antimonide with those in the other III-V semiconductors studied from this point of view of viz., InSb, InAs, InP, GaAs, GaSb, and GaP.[50] With the exception of aluminum antimonide and gallium phosphide, all these semiconductors have vanishingly small donor-ionization energies, evidently a consequence of the very small effective mass associated with the conduction-band minimum at $\mathbf{k}=0$. Evidence for bound donor states has been obtained for indium antimonide when the material was examined optically and electrically in high magnetic fields.[51–55] In the presence of a sufficiently high magnetic field, a finite binding energy for donors as well as localized states associated with Landau levels were observed. *Per contra*, both aluminum antimonide and gallium phosphide have conduction-band minima along the $\langle 100\rangle$ directions in $\mathbf{k}$ space. For aluminum antimonide the effective-mass parameters for these valleys are such that a large binding-energy results. In the case of gallium phosphide, evidence for the existence of bound donor states has recently been obtained by Dean *et al.*[56] who attribute many of the lines observed in the luminescence spectra to two electron transitions associated with the decay of excitons bound to neutral donors. It is of interest to note that large donor binding energies may occur in a semiconductor having its conduction-band minimum at $\mathbf{k}=0$ if the donor wave functions are associated primarily with higher-lying subsidiary minima characterized by large effective-mass parameters. An interesting example of this has been reported recently by Kosicki *et al.*[42] who have observed a donor level associated with sulfur impurities in gallium antimonide lying 75 meV below the conduction-band minimum at $\mathbf{k}=0$. They have deduced that this level is associated with the $\langle 100\rangle$ minima. Optical observations of such donor states have not yet been reported.

The photoexcitation spectra of tellurium and selenium donor electrons in aluminum antimonide are compared in Fig. 20. The contribution to the absorption in the tellurium spectrum due to the multiphonon lines L_{13}–L_{16} has been subtracted. In the figure, lines 4 and 5 in the selenium and tellurium spectra, respectively,

[50] O. Madelung, Ref. 28, Chap. 5, p. 224. See also D. V. Eddolls [Phys. Status Solidi **17**, 67 (1966)] who has studied the electrical properties of n-type epitaxial GaAs; he deduces an ionization energy of 5 meV at "infinite dilution" of donors.

[51] W. S. Boyle and A. D. Brailsford, Phys. Rev. **107**, 903 (1957).

[52] E. H. Putley, J. Phys. Chem. Solids **22**, 241 (1961).

[53] M. A. C. S. Brown and M. F. Kimmitt, Infrared Phys. **5**, 93 (1965).

[54] R. Kaplan, J. Phys. Soc. Japan Suppl. **21**, 249 (1966).

[55] R. J. Sladek, J. Phys. Chem. Solids **5**, 157 (1958).

[56] P. J. Dean, J. D. Cuthbert, D. G. Thomas, and R. T. Lynch, Phys. Rev. Letters **18**, 122 (1967).

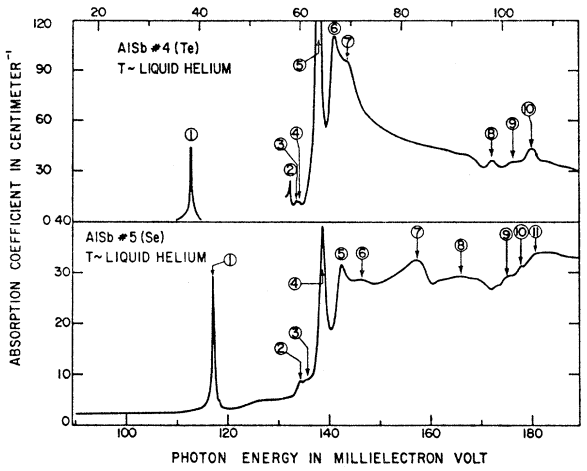

FIG. 20. Comparison of the excitation spectra of tellurium and selenium donors in aluminum antimonide. The lines attributed to the $1s(A_1) \rightarrow 2p_\pm$ transition in each case have been brought into coincidence. For the selenium-doped sample, $n(300°K) \simeq 10^{16}$ cm^{-3} and for the tellurium-doped sample, $n(300°K) \simeq 5 \times 10^{16}$ cm^{-3}. The absorption due to lattice bands has been subtracted in the absorption spectrum for tellurium donors.

have been brought into coincidence; both lines have been assigned to the $1s(A_1) \rightarrow 2p_\pm$ transition. As can be seen from both the figure and Table IV, the spacings between corresponding pairs of lines in the two spectra agree, within experimental accuracy, for the lines having $3p_\pm$, $2p_\pm$ and $3p_0$ for their final states. The $[2p_\pm - 2p_0]$ spacings are slightly different for the two donors, while the $[2p_\pm - 1s(T_1)]$ spacings differ by ~ 4 meV. Thus the equality of spacings between the excitation lines for the various donors in silicon and in germanium, which provides one of the most striking successes of the effective-mass theory for those materials, is not obtained for aluminum antimonide. Also, the agreement between the experimentally observed spacings and those calculated theoretically is not as good here as for the corresponding case of donors in silicon[7] and germanium.[31] This may arise both from deficiencies in the effective-mass theory as applied to aluminum antimonide and from the uncertainty in the values of the relevant effective-mass parameters. In addition, the experimentally observed relative intensity of the $1s(A_1) \rightarrow 2p_0$ with respect to the $1s(A_1) \rightarrow 2p_\pm$ transition in aluminum antimonide is much smaller than that observed for donors in silicon. On the other hand, both with regard to relative intensities and the number of lines clearly resolved, the donor spectra obtained by Dean *et al.*[56] in their luminescence measurements in gallium phosphide resemble the donor spectra in silicon much more closely than do those of selenium and tellurium donors in aluminum antimonide. Hence it is not obvious that the above mentioned differences between the donor spectra in aluminum antimonide and those in silicon can be explained by invoking the partially ionic character of the former. It could be argued that line 1 in each spectrum is actually due to a $1s(A_1) \rightarrow 2p_0$ transition, an assignment which is consistent with its stress behavior and its intensity relative to the lines ascribed to $1s(A_1) \rightarrow 2p_\pm$ transition. However, this interpretation leads to spacings completely out of line with the effective-mass calculations. This lack of agreement could be interpreted as due to less screening for some of the excited states than assumed in the effective-mass theory. At the present it is felt, however, that little is gained by this interpretation. Accepting the interpretation that line 1 in both the tellurium and selenium spectra can be attributed to the $1s(A_1) \rightarrow 1s(T_1)$ transition, and taking the ionization energies of the selenium and tellurium donors as 146.5 and 68 meV, respectively, one obtains a binding energy of ~ 30 meV for the $1s(T_1)$ level for each donor. The rather large difference between this value and the 40 meV predicted in the framework of the effective-mass theory using the static dielectric constant indicates that this theory must be improved upon in this respect. It is likewise important that the donor-ionization energies, particularly for selenium, should be determined with greater precision. Although the uncertainty in E_I(Se) prevents an accurate comparison of the binding energy of the $1s(T_1)$ state for selenium and tellurium impurities, the difference of 3.6 ± 0.5 meV between the $[2p_\pm - 1s(T_1)]$ spacings for tellurium and selenium donors may indicate a chemical species dependence for this state. In view of the low intensities of the $1s(A_1) \rightarrow 1s(T_1)$ transitions observed for bismuth-doped silicon,[33,35] the high intensities of line 1 relative to those of lines 4 and 5 of the selenium and tellurium spectra, respectively, are somewhat surprising.

It has been seen in the preceding sections that many of the peaks and shoulders observed at energies greater than the ionization energy in both the tellurium and selenium spectra can be interpreted as arising from electronic excitations accompanied by the emission of one or more phonons. It was noted in Sec. III that the relative intensity of line 5 in the tellurium spectrum with respect to its one-phonon replica, line 10, is of the order of magnitude expected if the electron-phonon interaction is assumed to arise either through optical deformation potentials or via the electrical-polarization field associated with the LO mode. It is probable that both mechanisms contribute to the transitions. This would be consistent with the observations of Stirn and Becker[57] that both polar- and nonpolar-optical mode scattering influence the mobility of electrons in aluminum antimonide at room temperature. In addition, the assumption of optical deformation potentials appears to be necessary to account for the participation of TO phonons in the excitation plus phonon transitions, since the TO modes do not interact with the electrons through their polarization fields. It should also be noted that lines 5 and 10 in the tellurium spectrum bear a marked resemblance to the lines associated with the $1s(A_1) \rightarrow$

[57] R. J. Stirn and W. M. Becker, J. Appl. Phys. 37, 3616 (1966).

$2p_{\pm}$ transition and the $1s(A_1) \rightarrow 2p_{\pm}$ transition accompanied by the emission of the LO_Γ phonon in the luminescence spectrum of excitons bound to neutral sulfur donors in gallium phosphide.[56]

Perhaps one of the most striking differences between the tellurium and selenium donor spectra is seen for energies greater than the donor-ionization energies (see Fig. 20). The absorption in the tellurium-doped aluminum antimonide falls off rapidly for energies greater than E_I(Te). In the selenium-doped material, however, there is a general increase of absorption for energies greater than $E_I(Se)$ up to $\sim$200 meV, beyond which there is a gradual decrease. This difference may be explained in part by the fact that excitation plus phonon transitions are expected to be much stronger for the selenium donors than for the tellurium donors assuming an electron-phonon interaction via either the optical deformation potential or the electric-polarization field associated with the LO phonons; this is a consequence of the much higher ionization energy for selenium donors than that for tellurium donors.[38,39]

The effects of uniaxial stress on the donor excitation lines of tellurium and selenium in aluminum antimonide have given valuable insight into the nature of the donor states. The absence of splitting for $\mathbf{F}\|\langle 111\rangle$ on the selenium donor spectrum is consistent with the deduction of Ghanekar and Sladek[26] that the lowest conduction-band minima lie along $\langle 100\rangle$. The fact that the lines do shift somewhat under stress implies, furthermore, that the various donor states shift by different amounts; this probably indicates the deficiency of the effective-mass theory as applied to aluminum antimonide. The possible consequences of piezoelectric effects have yet to be examined. The behavior of lines 1 and 2 in both donor spectra for all stress directions is consistent with their assignments to $1s(A_1) \rightarrow 1s(T_1)$ and $1s(A_1) \rightarrow 2p_0$ transitions, respectively, assuming the donor site symmetry to be T_d. Moreover, the observed splittings and polarization patterns indicate that the shear deformation potential for aluminum antimonide has the same sign as that for the conduction band of silicon; this is in agreement with the results of the piezoresistance measurements of Ghanekar and Sladek.[26] It has not been possible to understand the stress behavior of the excitation lines at energies greater than that of line 2 in the spectrum of either selenium or tellurium donors on the basis of any of the following models: an inverted ground state, with the $1s(A_1)$ level lying above the $1s(E)$ and $1s(T_1)$ levels as observed for isolated lithium donors in sliicon,[8] donor site symmetry different from T_d perhaps due to the existence of some type of donor complex as in the case of sulfur in silicon,[34] or donor wave functions with contributions from band extrema other than the $\langle 100\rangle$ minima of the lowest conduction band.[42] It is evident that samples of quality superior to those presently available should be measured in order to gain better resolution of the excitation lines 3, 4, 5. . . and to rule out the possible effects of overlapping wave functions of donor states.

In addition to the information discussed above, interesting new features for the lattice lines were observed in the course of investigating the donor excitation spectra. Of particular interest was the observation at low temperature of lines L_1, L_2 and L_3 on the long-wavelength side of the reststrahlen peak. It does not appear that these peaks are due to single-phonon creation in imperfect crystals since such transitions are usually observed in crystals having impurity concentrations orders of magnitude larger than those in the samples used in the present investigation.[58]

ACKNOWLEDGMENTS

The authors are indebted to Professor R. J. Sladek and Professor W. M. Becker for generously supplying some of the specimens used in the present investigation. They wish to thank Professor W. M. Becker, Professor P. Fisher, Professor E. W. Prohofsky, and Professor R. J. Sladek for enlightening discussions, Professor H. J. Yearian for orienting the samples, and Dr. A. Onton for the use of the computer program for data analysis.

[58] See, for example, J. F. Angress, A. R. Goodwin, and S. D. Smith, Proc. Roy. Soc. (London) **A287**, 64 (1965).